

# An Extended Geometric Approach in Active Vision to Detect and Eliminate Specularity in Shiny Colored Objects.

Pujitha Gunaratne \*

Yukio Sato #

Department of Electrical and Computer Engineering  
Nagoya Institute of Technology

## Abstract

In this paper we present an extended geometric approach, that detects and eliminates the specular points in a texture image of shiny objects, with the help of corresponding range data. The approach neither counts on spectral variations of the texture image nor employs rigid constraints on illumination sources, such as point light source limitations. It rather determines the candidate specular points, based on range data measured at the same view direction as the texture image, the viewing geometry, the geometry of the illumination source, and provides spatial information of such points to the secondary processing algorithms. The specular elimination process is embedded with a viewpoint shift algorithm, which uses an active vision methodology, based on data supplied by the geometric method.

## 1. INTRODUCTION

Construction of realistic 3-D models of objects has been sought in a variety of computer vision application areas ranging from computer graphics, CAD, virtual reality, electronic catalogues, and so on. 3-D model acquisition has been extensively discussed by the computer vision research community, and a number of approaches have been proposed in the past [1]. In this work we adopt an active vision oriented approach for 3-D model acquisition, which could be able to construct models of real world complex objects. Such a system has previously been demonstrated in [2], where a rangefinder called the "Cubicscope" is mounted on an articular robot arm with five degrees of freedom. It has been noted however, that the constructed model possesses with some undesirable texture variations due to the specularity in corresponding texture images.

There are a number of approaches proposed by various researchers to deal with highlights in texture images up to date. Most of such methods however have their own limitations or restrictions when applied to general cases. The dichromatic reflection model, proposed by Shafer et al. in [3], bears the application limitation for textures with almost similar spectral variations as the illumination source. In such cases, body and surface reflection clusters would almost coincide, thus making it hard to separate.

Other well known reflection models, such as Beckman, and Spizzichino [4], Cook and Torrance [5], ei-

ther contribute to the limitation of point light source restrictions or require extensive computations to track down specular spots in a texture image. Such limitations would adversely affect the needs of our system, which encourages a technique that could be implemented as an intermediate step to the said 3-D modeling task. Therefore the core of this study is devoted to finding a robust yet simply implementable highlight extraction method, which will be well suited as an intermediate task in an active vision oriented 3-D object modeling activity.

## 2. THE GEOMETRIC MODEL

As described in the previous section, the consideration is mainly based on constructing a simple, yet a robust technique, that extracts highlight components, which can be implemented as an intermediate processing step of the 3-D modeling system. Let us consider the geometry of highlight formation in a texture image, captured from a pin-hole camera (fig. 1).

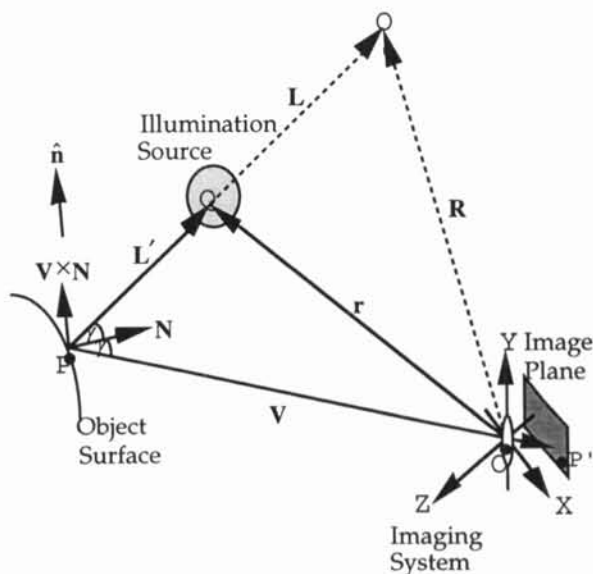


Fig. 1: Highlight formation at point P  
Hence considering the global surface reflection component, which would be visible as highlight in the image plane of a pin-hole camera, the necessary and sufficient condition for its formation can be stated as: the existence of a light beam, which is responsible for the specularity at any point P on the object surface, which

makes the specular spot  $P'$  on the image plane, emerges from any arbitrary point  $Q$  of the illumination source. Such a beam should make equi-angles with the surface normal drawn at point  $P$ , and with incident and reflected beams at that point. This phenomena of specularly formation is diagrammatically depicted in figure 1.

Lets assume the specular point  $P$  on the object surface, is observed as point  $P'$  on the image plane. Let  $X, Y, Z$  be the camera coordinates of the imaging system, with respect to which the distance  $P_x, P_y,$  and  $P_z$  are measured.

Let  $\mathbf{V}$  be the view vector or the surface reflection vector of  $P$ , in the direction of  $PO$ , and  $\mathbf{N}$  be the surface normal vector calculated at point  $P$ . Let  $\mathbf{L}'$  be the illumination vector, which originates from a point  $Q$  on the light source. Hence  $\mathbf{L}'$  and  $\mathbf{V}$  make equi-angles  $\gamma$  with  $\mathbf{N}$ . Therefore we can assume that  $\mathbf{V}, \mathbf{N}$  and  $\mathbf{L}'$  are co-planer. Also assume that  $\hat{\mathbf{n}}$  be a unit vector, which passes through the point  $P$ , and perpendicular to both  $\mathbf{V}$  and  $\mathbf{N}$ . Let  $\mathbf{L}$  be the vector generated by rotating  $\mathbf{V}$  in an orthogonal plane around  $\hat{\mathbf{n}}$  by a positive angle  $2\gamma$ . Hence we can derive the vector  $\mathbf{L}$ ;

$$\mathbf{L} = \mathbf{V} \cos 2\gamma + (\hat{\mathbf{n}} \times \mathbf{V}) \sin 2\gamma, \text{ or}$$

$$\mathbf{R} = (\hat{\mathbf{n}} \times \mathbf{V}) \sin 2\gamma - (1 - \cos 2\gamma) \mathbf{V},$$

where  $\mathbf{R}$  is the position vector of  $O''$ . Since  $\mathbf{L}$  and  $\mathbf{L}'$  are co-linear;

$$\mathbf{L}' = \lambda \mathbf{L} \quad \text{----- (1)}$$

for any scalar  $\lambda > 0$ . We can show that the scalar factor  $\lambda$  is light source geometry dependent, and can be derived for different sources, once the geometry is known [6]. Hence from the calculation of  $\mathbf{L}'$  for every point  $P$  on the object surface, and the knowledge of the light source geometry, we can determine whether  $\mathbf{L}'$  passes through the light source. Therefore a core requirement of this method lies on the mathematical derivation of the light source geometry.

In most of the real world applications, it is observed that the illumination sources have a symmetric geometry, hence possess an axis of revolution. Such symmetric surfaces can easily be modeled with finite vector functions in the form of  $\mathbf{F}(\mathbf{r}, \hat{\mathbf{u}}, \xi)$ , where  $\mathbf{r}$  is the position vector of any point on the surface,  $\hat{\mathbf{u}}$  is a unit vector along the symmetric axis and  $\xi$  is any surface dependent scalar constant.

Hence, with the implementation of this vector function approach, we can determine whether  $\mathbf{L}'$  satisfy the vector function defined for the illumination source employed. If such a situation satisfies, then the corresponding points  $P$  on the object surface can be considered as the probable candidate points of specularity. Here we make the assumption that the illumination source consist of a constant irradiance over the total extent of area where the vector function is defined. In this experiment, a flat symmetric ring light source is used, merely to simplify computations and due to the

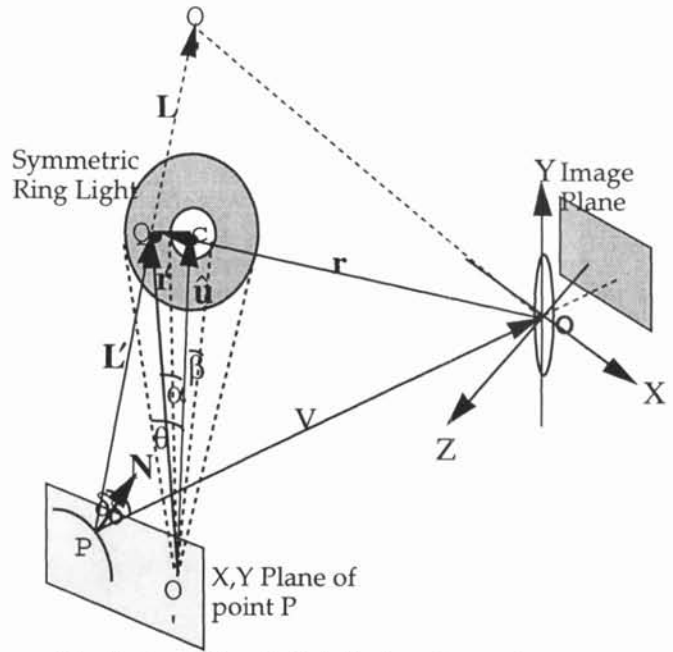


Fig. 2: Use of ring light in the imaging system ability of easy mounting to our system. The vector function of such a source can be easily defined as vector products. The geometry of such a system is depicted in the figure 2.

The vector function of the light source surface with respect to the origin  $O'$  can be derived, in the form of vector products as:

$$(\mathbf{r}' \cdot \hat{\mathbf{u}})^2 = \cot^2(\alpha + \beta) [\hat{\mathbf{u}} \times (\mathbf{r}' \times \hat{\mathbf{u}})] \quad \text{----- (2)}$$

where  $\mathbf{r}'$  is the position vector of  $Q$  with respect to  $O'$ . To simplify calculations we bring the light source in front of the imaging system in such a way that the light source is  $Z_s$  distance away from the optical center and its symmetric axis is parallel to the  $Z$  axis, which passes through the optical center  $O$ . With this configuration,  $\lambda$  can be modeled as;

$$\lambda = \frac{Z_s + V_z}{L_z},$$

where  $V_z$  and  $L_z$  are  $Z$  values (depth) of vectors  $\mathbf{V}$  and  $\mathbf{L}$  respectively [6]. Hence  $\mathbf{L}'$  and subsequently  $\mathbf{r}'$  can be evaluated. Therefore if  $\mathbf{r}'$  satisfies the equation (2), for any  $\alpha$  where,

$$0 \leq \alpha \leq (q - b)$$

the corresponding points  $P$  on the surface are considered to be the probabilistic specular points[6].

### 3. SPECULAR DATA REFINEMENT

Once the probabilistic specular data is extracted by the geometric method, we apply further refinement algorithms to prune such data due to the presence of possible noise in range data. Although we employ a median average algorithm to the raw range data, before applying the geometric method, we cannot ignore the effect caused by such noisy data towards the extracted specular points, due to their high sensitivity to the surface

normal. Therefore we apply two types of refinement algorithms to compensate such effects and extract only the highest probabilistic data points.

### 3.1 Neighborhood Refinement

The first algorithm, neighborhood refinement, can be viewed as a "merge or drop" algorithm, which operates on a pre-defined heuristic value. Before its application, first we mark the selected specular points from the geometric method as candidate points with voting 1. Then a mask of a known size is applied through all the points of the image and look for other candidate points. With the detection of such points, all the surrounding neighbors are scanned. If the neighbors do satisfy the pre-defined heuristic (20%, 30%, 50% etc.), in other words, if there is a good percentage of neighbors that satisfy the set heuristic, around the current data point, then the current point is voted as specular point (100% votes). If not (heuristic not satisfied), the candidature of the current point is removed (votes set to 0). The value of the heuristic is directly depend on the mask size of the median filter. Hence we can merge all the undetected specular points around detected ones, while dropping false detected ones at the same time, as shown in the figure 3.

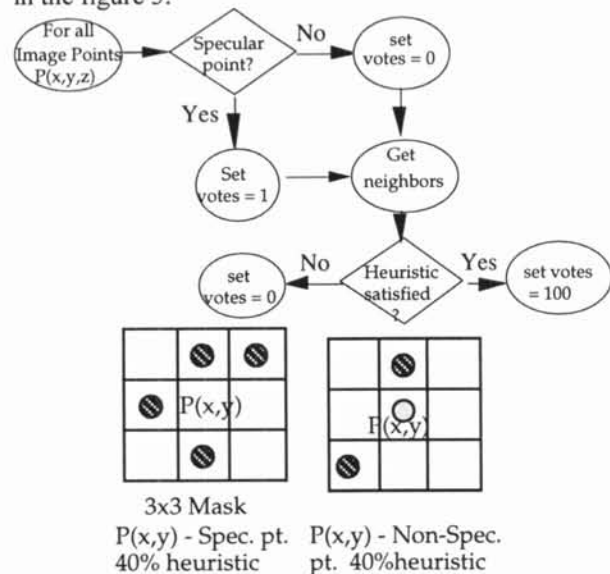


Fig. 3: Neighborhood Refinement

### 3.2 Spectral Refinement

Upto now we have been considering the physical formation of highlight component with respect to the shape of the object surface. Once the candidate points are extracted by the neighborhood refinement algorithm, we check the spectral compositions of those points to check for further integrity for specularity. Such a secondary refinement, the spectral refinement, is done to eliminate the remaining anomalies, especially due to the prominent noises at the edges of range data. A threshold is set for the R, G, B indexes of the texture image, depending on the highest and lowest R, G, B values that were reported, and thus the pixels below the set threshold will be discarded (fig. 4).

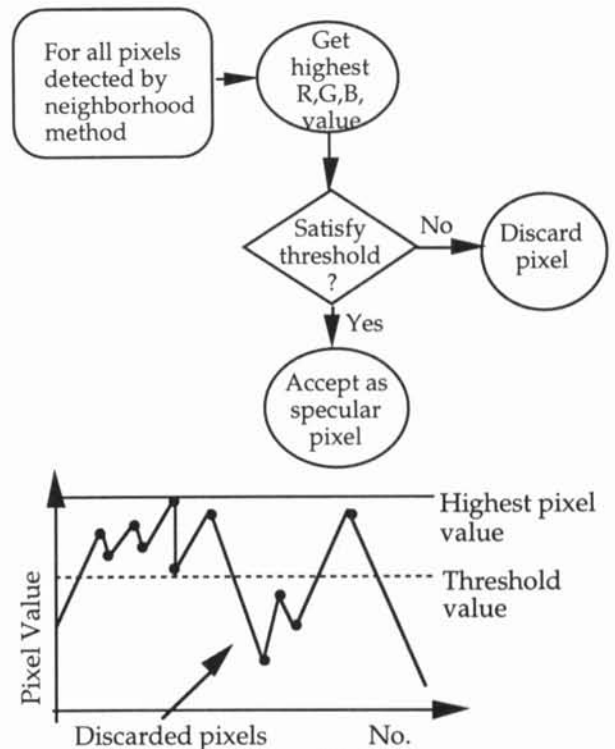


Fig. 4: Spectral Refinement

It should be noted however, that the role of spectral refinement plays a local processing activity rather than a global highlight extraction process, in that data points input to spectral refinement are those qualified by the geometric method and the neighborhood refinement. Hence this technique can be well applied to surfaces with varying spectral compositions.

## 4. SPECULAR ELIMINATION

Once we have pruned the candidate domain of specularity by above methods, the rest is to extract highlights from the detected locations and replace with corresponding texture information of the object surface. For this purpose, we construct a "Geodesic dome", which is the trace of the robot manipulator in 3-D space, when measuring the object. We divide the geodesic dome into triangular patches of which any given set of points on the object surface contribute to a unique projection to each patch (fig. 5).

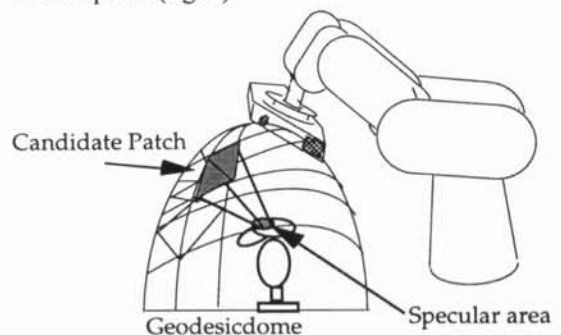


Fig. 5: Candidate patches of specular points.

Once the present viewpoint is registered, all the candidate patches contributed by the extracted specular

points are traced on that view point. From the surface normal ( $N$ ), view direction vectors ( $V$ ), and light source direction vectors ( $L'$ ) at each specular points, the probabilistic cone for maximum specularity detection is constructed. Then the manipulator is moved to the next best view location, avoiding previously detected specular patches.

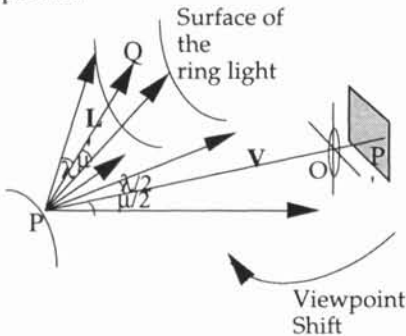


Fig. 6 View point shifting against maximum reflection angle.

The manipulator movement routine is also incorporated with measuring routine of the next unmeasured area, in that, the manipulator is moved to the next best viewpoint to measure range data of the unmeasured object area, as well as acquire specular free texture data of the previous specular points. This is achieved by posting the edge boundaries (of jump edges), from range data, as well as specular data on to the dome patches. Then the previous specular coordinates are transformed to the new view coordinated and corresponding specular free data is extracted. Hence eliminate the previous specular points by replacing with new values. We also perform a local brightness adjustment with the surrounding pixels to the new texture pixels, before replacing for specular points, to avoid patch like appearance.

## 5. EXPERIMENT RESULTS

In this section we present the results of specular elimination of a toy bird model.

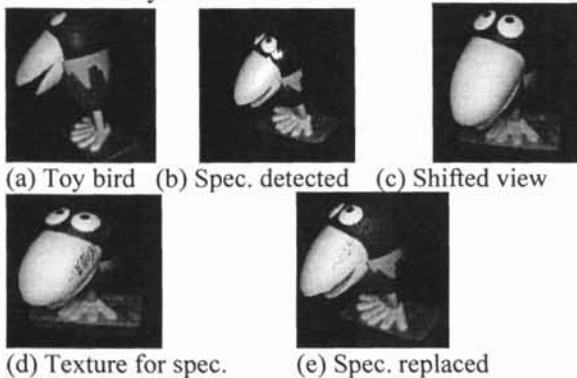


Fig. 7: Specular extraction for a toy bird.

Figure 8 shows the elimination range of pixels by the spectral refinement, detected previously by the geometric and neighborhood methods.

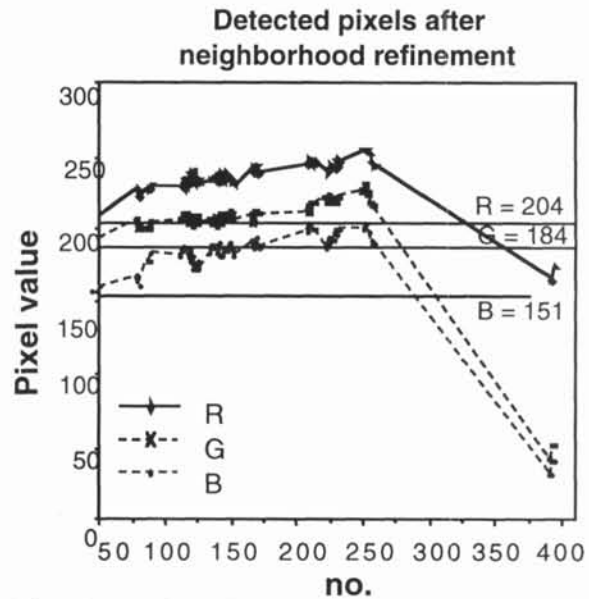


Fig.8: Spectral scrutiny for neighborhood refined pixels

## 6. CONCLUSION

We have presented a highlight extraction technique that has been implemented in an active vision environment. The prime goal of this work is to construct a simple yet robust technique of highlight extraction, to be implemented as a co-routine with 3-D object modeling applications. The proposed model neither need an a priori segmentation information nor count on spectral variations to detect highlight components. However this method relies on the existence of range data and construction of a finite vector function of the illumination source.

## 7. REFERENCE

1. X. Yuan, A Mechanism of Automatic 3D Object Modeling, IEEE Trans. on Patt. Analy. and Mac. Intl. Vol. 17, No.3, March 1995.
2. M. Otsuki, Y. Sato, Active 3-D Shape Reconstruction by Cubicscope, ACCV'93, November 23-25, Osaka, Japan.
3. G.J. Klinker, S.A. Shafer, T. Kanade, The Measurement of Highlights in Color Images, Intl. Jour. of Comp. V., 2, 7-32, 1988.
4. P. Beckmann, A. Spizzichino, The Scattering of Electromagnetic waves from Rough Surface, Mac-Millan, New York, 1963, pp. 1-33, 70-96.
5. R. L. Cook, K. E. Torrence, A Reflectance Model for Computer Graphics, Comp. Graphics, 15 (3) 307-16.
6. P. Gunaratne, Y. Sato, Application of an Extended Geometric Approach to Detect and Eliminate Specularities in Shiny Objects using Active Vision, Technical Report of IEICE, PRMU98-05.